Parametric Study of Slender Shear Walls Reinforced with Shape Memory Alloy Bars

Deepak Saud, Lisa Tobber, and M. Shahria Alam

Abstract In mid-rise and high-rise buildings, reinforced concrete (RC) shear walls are frequently used to resist seismic forces in earthquake-prone countries. The post-earthquake repair and retrofitting of these walls are very expensive or uneconomical, as observed in the 2010 Chile and 2011 Christchurch earthquakes. This paper explores the use of shape memory alloy (SMA) bars in the plastic hinge region of slender reinforced concrete (RC) shear walls. A comprehensive numerical parametric study was performed to understand the effects of various parameters on the hysteretic (force–deformation) response. Several models were developed with different aspect ratios, axial load ratios, reinforcement ratios, and types of SMA. The walls were then subjected to axial and reverse cyclic lateral loading, and the responses were assessed. Based on the responses, new trends were identified between design parameters and response outputs such as stiffness, residual deformation, force–deformation, and critical damage states (i.e. cracking, yielding, and crushing of SMA RC walls). These new relationships can be used to inform the design of low damage SMA RC walls for high seismic regions in Canada and worldwide.

Keywords Parametric study · Shear wall · Shape memory alloy · Axial and cyclic loading · Numerical modelling

1 Background and Introduction

One of the most common lateral force resisting systems in mid-rise and high-rise buildings is reinforced concrete shear walls (referred to herein as *shear walls*). In addition to resisting earthquake and wind loads, shear walls also support gravitational loads. Under strong earthquake shaking, these shear walls are designed for life safety, where the building can endure heavy damage. Past earthquakes have shown that buildings designed to this criterion underwent severe damage, particularly in

D. Saud (✉) · L. Tobber · M. S. Alam
The University of British Columbia, Kelowna, Canada
e-mail: dsaud@student.ubc.ca

R. Gupta et al. (eds.), *Proceedings of the Canadian Society of Civil Engineering Annual Conference 2022*, Lecture Notes in Civil Engineering 359,
https://doi.org/10.1007/978-3-031-34027-7_4

many mid-rise and high-rise reinforced concrete buildings [8, 9]. The post-earthquake repair and retrofit of these buildings are expensive or uneconomical. Therefore, shear walls should be designed to minimize damage to these structural elements, resulting in low or no permanent deformation in the buildings. One alternative is to use superelastic shape memory alloy (SMA) bars at the critical locations (plastic hinge regions) of the shear walls in lieu of typical steel reinforcing [14].

SMA is an innovative material that has a superelastic property. This material can return to its initial shape and position after removing the loading on the structure [3]. The SMA demonstrates superelasticity behaviour when it is in the austenite state. In addition to the superelasticity property, SMA has a very low or negligible residual strain after unloading. Moreover, SMA can dissipate substantial energy during repeated load cycles. Therefore, SMA material has significant potential for civil engineering applications to make structures seismic-resistant in earthquake-prone areas.

Figure 1 shows the stress–strain behaviour of SMA under reversed cyclic lateral loading at a constant temperature. When stress is applied to SMA, the material changes its form from austenite to a martensite state. The transformation can be represented by four parameters, namely austenite-to-martensite starting stress (f_y), austenite-to-martensite finishing stress (f_{P1}), martensite-to-austenite starting stress (f_{T1}), and martensite-to-austenite finishing stress (f_{T2}).

The self-centring system developed with SMA in shear walls can reduce permanent deformations and damages. This reduction in damage could avoid the demolition and reconstruction of structures in high seismic areas. Therefore, although the SMA bars are expensive compared to the steel reinforcement, they are economical in the long term when used at the plastic hinge regions of the shear walls.

The superelastic SMA is connected with steel rebars by mechanical couplers. SMA rebars were successfully implemented in the plastic hinge regions of SMA RC elements by various researchers [11, 12, 17]. However, only a few studies have been

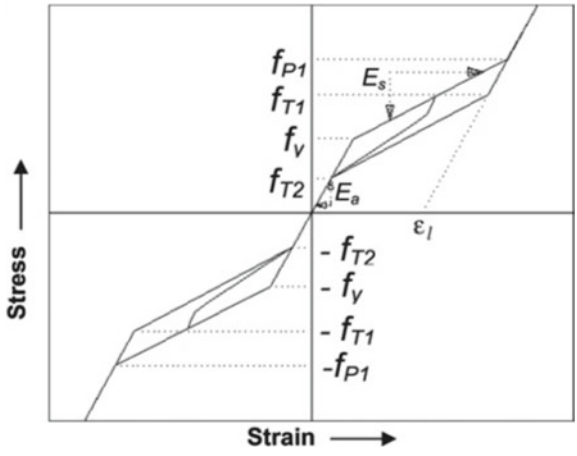

Fig. 1 1D superelastic model of SMA incorporated in FE packages (adapted from Auricchio et al. [5])

conducted on SMA bars as potential reinforcements in the plastic hinge regions of shear walls [1, 4, 7, 15].

In previous experimental tests conducted on SMA RC walls, the specimens were limited to axial load forces less than 4% $f_c' A_g$ and aspect ratios (length to height ratio of a shear wall) between 1 and 2.2 because of the laboratory size and equipment availability. Most of these tests were only tested under quasi-static lateral loading, except the test done by Almeida et al. [4], in which the walls were tested under both axial and quasi-static loading. Further, most experimental tests showed overturning due to axial load less than 3%, except the test done by Almeida et al. [4], which had 81%. Table 1 provides the detail of experimental tests conducted in recent years on shear walls connected with SMA bars.

In Table 1, the aspect ratio is the ratio of the height of the wall (h_w) to the length of the wall (l_w), P is the axial load including self-weight of the wall, f_c' is the concrete cylinder compression strength, A_g is the cross section of the wall, and V is the peak force observed during the test.

Due to the lack of literature on the experimental testing of SMA RC shear walls, there is a significant knowledge gap in understanding the behaviour of shear walls with SMA in their plastic hinge regions. Most shear walls have an axial load ratio between 5 and 10% in real buildings. Therefore, it is critical to determine the behaviour of SMA RC walls made of higher aspect ratios under varying axial loading (5 and 10%).

The present study explores the potential use of SMA bars in slender reinforced concrete (RC) shear walls. A comprehensive numerical parametric analysis was performed to understand various parameters' effects on the hysteretic (force–deformation) response. The critical parameters analysed were aspect ratio, axial load ratio, types of rebars, and vertical reinforcement ratio. Several finite element models were developed using these parameters. The walls were then subjected to axial and reverse cyclic lateral loading for assessing the response. Finally, the results obtained from this numerical study will lead to an experimental testing programme for slender SMA RC shear walls.

Table 1 List of experimental tests conducted on SMA RC shear wall

Experimental tests	Aspect ratio (h_w/l_w)	Axial load ratio ($P/f_c' A_g$) (%)	$V/A_g/f_c'$ (%)	$Pl_w/2Vh_w$ (%)
Almeida et al. [4]	1.7	3.83	1.43	80.52
Kian et al. [15]	2	0.08	1.84	1.05
Abdulridha et al. [1]	2.2	0.17	2.81	1.35
[7]	2.2	0.07	1.13	1.31
Cortés-Puentes [7]	1	0.19	4.31	2.25
	1	0.18	7.75	1.13

2 Parametric Analysis

A parametric analysis was performed to understand the cyclic response of SMA bars compared to steel rebar. The most appropriate type of SMA observed for structural applications is NiTi due to its ability to recover considerable strain, superelasticity, and excellent corrosion resistance [3]. FeMnAlNi alloy developed by Omori et al. [10] exhibits superelasticity in the range of NiTi, but at a low austenite finish temperature. This enables FeMnAlNi to function in the superelastic range even at a low temperature [6]. The SMA properties shown in Table 2 were referenced from the studies of [3, 10].

The parametric study considered three aspect ratios, three different rebar types (steel, NiTi, FeMnAlNi), two axial load ratios ($P/f_c'A_g$), and three different vertical reinforcing ratios (ρ_v). A total of 54 walls were analysed ($3 \times 3 \times 3 \times 2 = 54$ models) under cyclic loading. A constant cross section of 150 mm thick and 1200 mm long was considered for all shear wall models. This cross section was selected as per the capacity at the structure's laboratory at the University of British Columbia, Okanagan Campus. Three different types of rebars—steel ASTM A706 Grade 60, NiTi and FeMnAlNi, of size #3, #5 and #7 were varied in the concentrated zones of the shear wall. In this study, the vertical reinforcement ratio (ρ_v) was taken as the longitudinal reinforcement ratio of only one portion of the concentrated zone, shown in Eq. 1.

$$\rho_v = \frac{4(\text{Area of rebar})}{150\,\text{mm} \times 210\,\text{mm}} \times 100\%. \tag{1}$$

The #3 steel rebars were provided as longitudinal and transverse rebars in the wall web for all models. Figure 2 shows the cross section of the shear wall and reinforcement detailing. Table 3 shows the parameters studied.

Table 2 Properties of SMA

Properties	NiTi	FeMnAlNi
Modulus of elasticity (E)	62.5 GPa	68 GPa
Austenite-to-martensite starting stress (f_y)	401 MPa	435 MPa
Austenite-to-martensite finishing stress (f_{P1})	510 MPa	535 MPa
Martensite-to-austenite starting stress (f_{T1})	370 MPa	335 MPa
Martensite-to-austenite finishing stress (f_{T2})	130 MPa	170 MPa
Superelastic plateau strain length (ε_1)	6%	8%

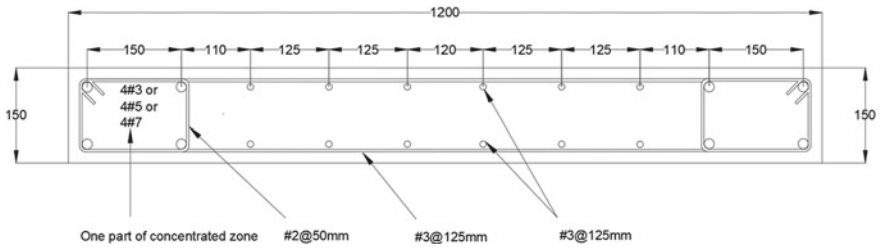

Fig. 2 Cross section of wall model

Table 3 Parameters to study

Parameters		Value		
a	Aspect ratio (h_w/l_w)	2	3	4
b	Axial load ratio ($P/f'_c A_g$)	5%		10%
c	Types of rebars	Steel ASTM A706 Grade 60	NiTi	FeMnAlNi
d	Vertical reinforcement ratio (ρ_v)	0.89%	2.48%	4.86%

3 Numerical Modelling

Two-dimensional finite element models of the shear walls were developed using Seismostruct software [13]. The inelastic displacement-based frame element type was selected to model the walls. The nonlinear behaviour of concrete and steel was modelled by the Mander model (1988) and Menegotto and Pinto model (1973). The SMA material was modelled with the available Auricchio and Sacco model (1997) in Seismostruct. Static time-history analysis was performed to simulate the quasi-static behaviour of shear walls under axial load and cyclic loading. The compressive strength of concrete and the yield strength of steel was taken as 56 MPa and 470 MPa, respectively [16].

The height of the various models was raised as per the aspect ratios of 2, 3, and 4. The bottom of the wall was fixed. The reverse cyclic lateral loading which incrementally increases the drift amplitude was used as shown in Fig. 3. The loading protocol was referenced from the study of [4]. Further, the loading protocol was also selected as per the capacity of horizontal and vertical actuators available in the laboratory. A vertical load of $0.05A_g f'_c$ or $0.1A_g f'_c$ was applied at the top with the reversed cyclic lateral loading in the shear wall models as shown in Fig. 4.

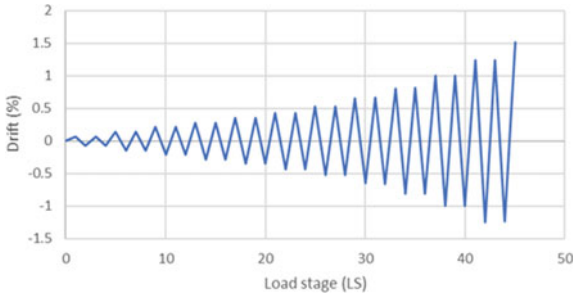

Fig. 3 Applied loading protocol

Fig. 4 Numerical model

4 Result

A model was developed for each of the 54 combinations, and each model was analysed under cyclic loading. The combination was named *R*#*A*#*P*#, where R = rebar size, A = aspect ratio, and P = axial load ratio. For instance, *R*3*A*3*P*5 represents rebar size #3, aspect ratio 3, and axial load ratio 5%.

4.1 Hysteretic Response and Trends

While assessing the various hysteretic responses for steel, NiTi and FeMnAlNi, interesting trends were observed. These trends are shown in Figs. 5, 6, and 7. From the hysteretic plots, it can be observed that there is a significant difference in the hysteretic shapes of steel and SMA (NiTi and FeMnAlNi) shear walls. Generally, the shear walls with only steel reinforcing showed larger hysteresis "loops" and, for the majority of models, had residual deformations. Contrastingly, the SMA models had

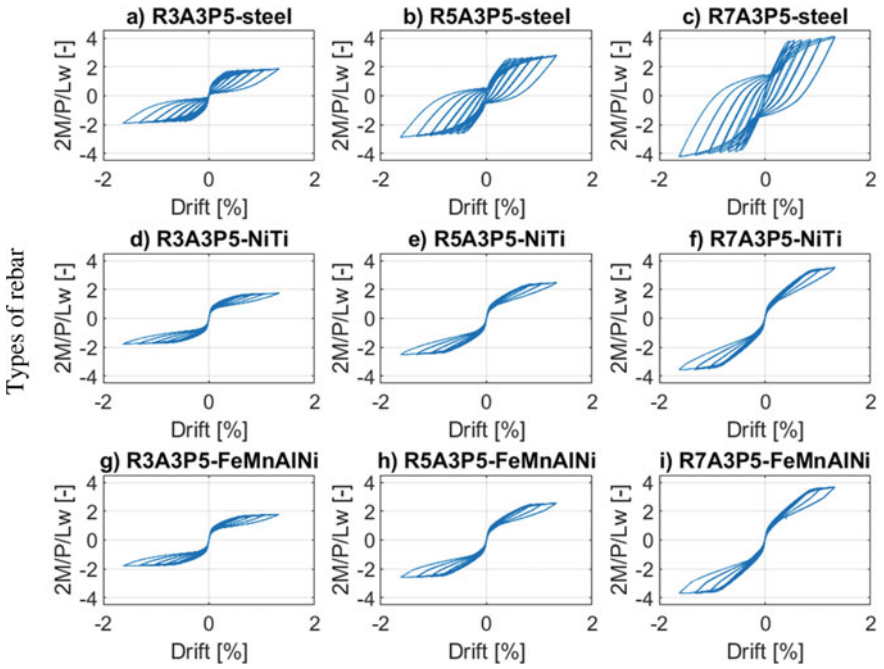

Fig. 5 Hysteresis trend for same aspect ratio and axial load ratio with varying rebar size (R = rebar size; A = aspect ratio; P = axial load ratio)

limited energy dissipation but showed minimal residual displacements, showcasing the SMA's excellent self-centring capabilities.

Figure 5 shows the different hysteresis for different vertical reinforcement ratios, a constant aspect ratio ($A = 3$), and a constant axial load ratio ($P/A_g/f_c' = 5\%$). In all cases, an increase in vertical reinforcement resulted in an increase in an overturning moment. In the steel models, a higher reinforcing ratio resulted in higher residual drifts. On the other hand, the SMA walls had low residual drift for all reinforcing ratios.

Figure 6 shows the different hysteresis for different aspect ratios, a constant reinforcing ratio of 2.48% (for rebar size #5), and axial load ratio ($P/A_g/f_c' = 5\%$). In all cases, a higher aspect ratio results in lower stiffness. Increasing the aspect ratio does not increase the capacity. Generally, a lower aspect ratio resulted in more energy dissipation (larger hysteretic loops) than a high aspect ratio.

Figure 7 shows the different hysteresis for different axial load ratio ($P/A_g/f_c' = 5\%$ and 10%), a constant reinforcing ratio of 2.48% (for rebar size #5), and aspect ratio ($A = 3$). Generally, increasing axial load resulted in a more pinched hysteresis (i.e. more prominent self-centring capability). However, a higher axial load led to earlier degradation of strength compared with a low axial ratio.

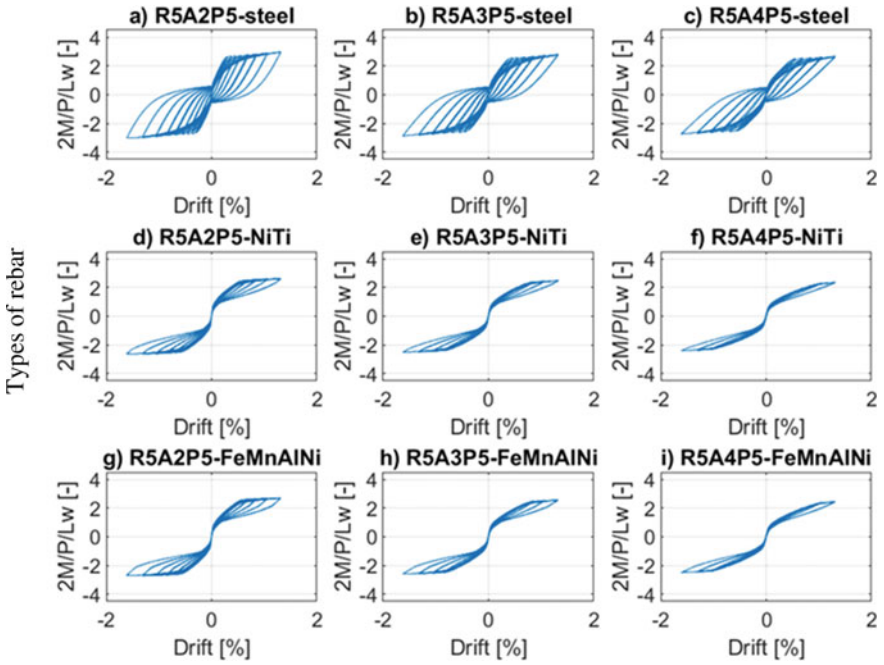

Fig. 6 Hysteresis trend for same rebar size and axial load ratio with varying aspect ratio (R = rebar size; A = aspect ratio; P = axial load ratio)

4.2 General Response

The residual drift is vital to determine the severity of damage to buildings after an earthquake. For this study, residual drift is taken as the ratio of permanent deformation over the height of the wall. Figure 8 shows the relationship between residual drift and vertical reinforcement ratio for steel, NiTi and FeMnAlNi at 5 and 10% axial load ratios.

As shown in Figs. 8a and d, residual drift was observed for all steel shear walls except for specimens with a reinforcing ratio of 0.89% ($R3$) and axial load ratio of 5%, where no residual drift was observed. Generally, an axial ratio of 10% had higher residual drifts than the axial ratio of 5%. The trend for the axial ratio of 5% walls showed that high vertical reinforcing ratios resulted in high residual drift. On the other hand, at an axial ratio of 10% walls with high vertical reinforcing ratios resulted in lower residual drift, except for $R5A4P10$, where the residual drift was low. In both axial ratios of 5% and the axial ratio of 10%, walls with a higher aspect ratio had lower residual drifts.

The SMA materials for an axial ratio of 5% showed no residual drift (i.e. Fig. 8b and c). On the other hand, the axial load ratio of 10% showed small residual drifts at the lower reinforcing ratios (i.e. Fig. 8e and f). The highest residual drift for SMA

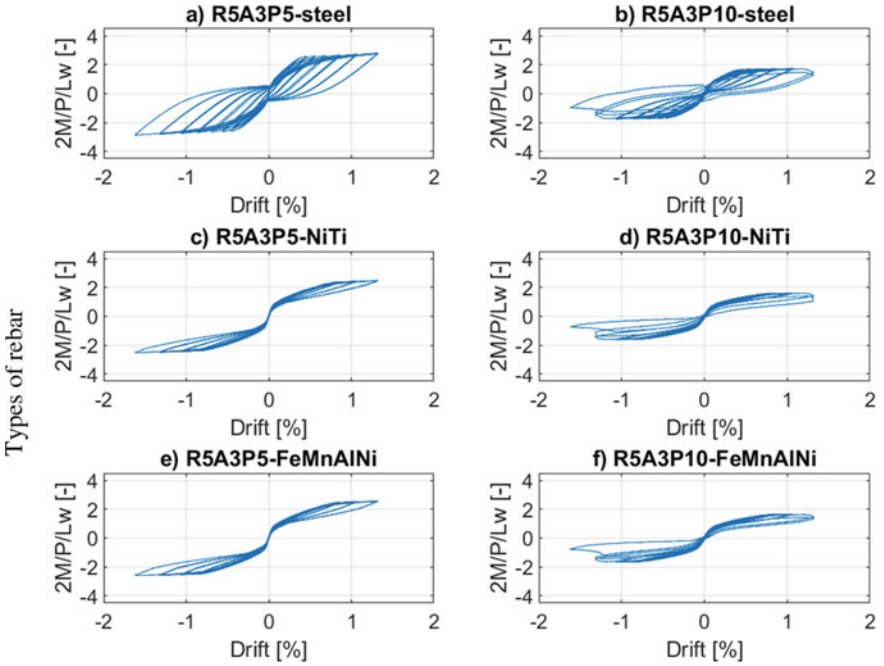

Fig. 7 Hysteresis trend for same rebar size and aspect load ratio with varying axial load (R = rebar size; A = aspect ratio; P = axial load ratio)

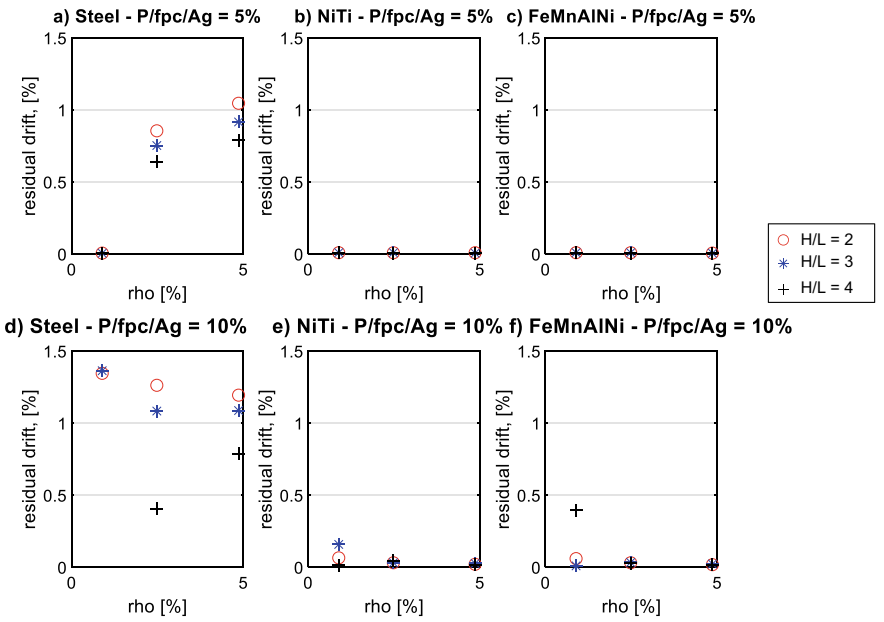

Fig. 8 Residual drift versus vertical reinforcement ratio

walls was about 0.2% for aspect ratio 3 specimen at a 0.89% reinforcement ratio. On the other hand, the highest residual drift for steel walls was observed at around 1.4% for all three varying aspect ratios specimens.

Energy is the accumulation of hysteretic energy (i.e. inelastic force–deformation response) over all the cycles, which is normalized by the maximum shear force (V_{max}) and the maximum displacement (Δ_{max}). The normalized energy (Energy/V_{max}/Δ_{max}) was used to show energy dissipation capacity.

Figure 9 shows that the normalized dissipated energy for steel is higher than the NiTi and FeMnAlNi at 5 and 10% axial load ratios. For steel, energy dissipation was increased with the high reinforcement ratio. In contrast, there was low energy dissipation for shear walls with a high aspect ratio.

Shear walls with NiTi and FeMnAlNi bars showed low energy dissipation for high reinforcement ratios, as shown in Fig. 9b, c, e, and f. The energy dissipation capacity of NiTi was slightly lower than the FeMnAlNi. Overall, the NiTi and FeMnAlNi showed less than half of the energy dissipation than steel.

The cyclic degradation rotation ($\theta_{80\%}$) is the drift when the shear force is degraded to 80% of the maximum shear force. The value of $\theta_{80\%}$ is important as it represents the system ductility, which is a critical design parameter. For a 5% axial load ratio, no strength loss was observed in all three types of rebars. However, strength loss was observed for a 10% axial load ratio. Figure 10 shows the drift when the force degraded to 80% of the peak force. For a 10% axial load ratio, a higher reinforcing

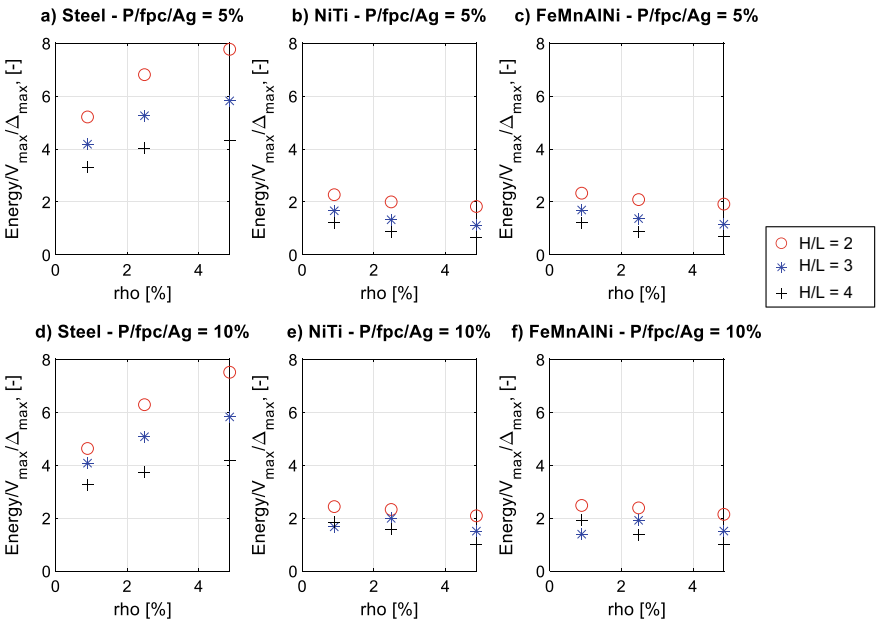

Fig. 9 Normalized energy dissipation versus vertical reinforcement ratio

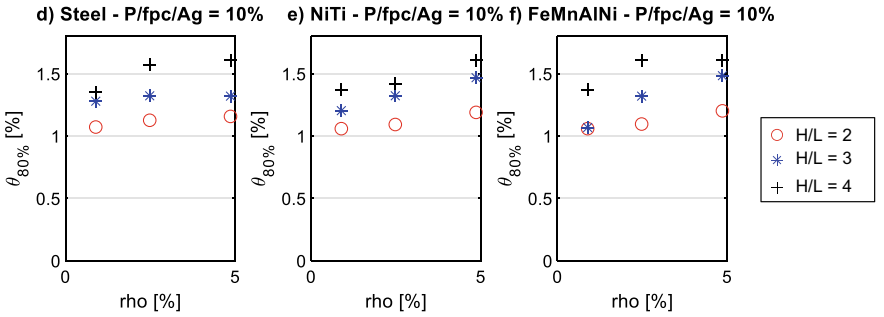

Fig. 10 Drift at strength loss ($\theta_{80\%}$) versus vertical reinforcement ratio

ratio resulted in a higher $\theta_{80\%}$. Furthermore, higher rotation values were observed for the higher aspect ratios.

The critical damage states (cracking, spalling, yielding, crushing) were analysed and shown in Fig. 11 with the help of boxplots. This was performed by the rotation distribution to four performance limit states to see the effect of various parameters. For NiTi and FeMnAlNi, the spalling of the concrete cover was observed before yielding the SE SMA rebars. This behaviour is because the SMA rebars effectively resist the forces after cracking. A similar observation was also observed in a previous study conducted by Billah and Alam [6] and Ahmad and Shahria Alam [2]. The median rotation value of yielding for NiTi and FeMnAlNi was more than twice the value of steel. Similarly, the median rotation value of crushing was observed at 1.2 for NiTi and FeMnAlNi, while it was observed at 0.98 for steel.

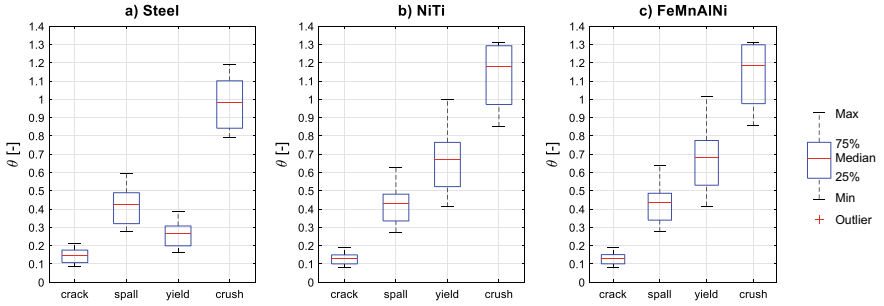

Fig. 11 Boxplot for critical damage states

5 Summary and Conclusion

A detailed parametric study was performed with the force–deformation response and strain obtained from 54 models. The major conclusions drawn from the study are as follows:

- There is a lack of availability of experimental data due to the limited test on SMA RC shear walls.
- The NiTi and FeMnAlNi reinforced shear walls showed minimal residual displacements, demonstrating SMA's excellent self-centring capabilities.
- Significant residual drift was observed for steel shear walls except at a reinforcement ratio of 0.89% and axial load ratio of 5%. In contrast, it was observed very low to none in NiTi and FeMnAlNi.
- The NiTi and FeMnAlNi showed less energy dissipation than steel-reinforced shear walls at 5 and 10% axial load ratios.
- No strength loss was observed at 5% axial load ratio for all three rebar types. However, strength loss was observed for a 10% axial load ratio.
- The spalling of the concrete cover was observed before yielding in NiTi and FeMnAlNi because of SMA's excellent capacity to resist the forces after cracking.

6 Future Work

A comprehensive literature review showed little experimental data is available on slender shear walls connected with SMA rebars. This study showed the excellent self-centring capacity of NiTi and FeMnAlNi shear walls. Further, very low residual drift was observed for NiTi and FeMnAlNi. However, experimental work is needed to further explore the appropriate detailing methods for SMA shear wall. Therefore, for future research, an experimental study of slender shear walls connected with shape memory alloy bars can be conducted based on this parametric study.

References

1. Abdulridha A, Palermo D (2017) Behaviour and modelling of hybrid SMA-steel reinforced concrete slender shear wall. Eng Struct 147:77–89
2. Ahmad N, Shahria Alam M (2015) Damage states for concrete wall pier reinforced with shape memory alloy rebar. In: The 11th Canadian conference on earthquake engineering
3. Alam MS, Youssef MA, Nehdi M (2008) Analytical prediction of the seismic behaviour of superelastic shape memory alloy reinforced concrete elements. Eng Struct 30(12):3399–3411
4. Almeida JP, Steinmetz M, Rigot F, de Cock S (2020) Shape-memory NiTi alloy rebars in flexural-controlled large-scale reinforced concrete walls: experimental investigation on self-centring and damage limitation. Eng Struct 220:110865
5. Auricchio F, Taylor RL, Lubliner J (1997) Shape-memory alloys: macromodelling and numerical simulations of the superelastic behaviour. Comput Methods Appl Mech Eng 146(3–4):281–312

6. Billah AHMM, Alam MS (2016) Performance-based seismic design of shape memory alloy–reinforced concrete bridge piers. I: development of performance-based damage states. J Struct Eng 142(12). American Society of Civil Engineers (ASCE)
7. Cortés-Puentes L, Zaidi M, Palermo D, Dragomirescu E (2018) Cyclic loading testing of repaired SMA and steel reinforced concrete shear walls. Eng Struct 168:128–141
8. Elwood KJ (2013) Performance of concrete buildings in the 22 February 2011 Christchurch earthquake and implications for Canadian codes. Can J Civ Eng 40(8):759–776
9. Jünemann R, de la Llera JC, Hube MA, Vásquez JA, Chacón MF (2016) Study of the damage of reinforced concrete shear walls during the 2010 Chile earthquake. Earthq Eng Struct Dyn 45(10):1621–1641
10. Omori T, Ando K, Okano M, Xu X, Tanaka Y, Ohnuma I, Kainuma R, Ishida K (2011) Superelastic effect in polycrystalline ferrous alloys. Science 333(6038):68–71
11. Saiidi MS, Wang HY (2006) Exploratory study of seismic response of concrete columns with shape memory alloys reinforcement. ACI Struct J 103:436–443
12. Saiidi MS, Sadrossadat-Zadeh M, Ayoub C, Itani A (2007).Pilot study of behavior of concrete beams reinforced with shape memory alloys. J Mater Civ Eng 19(6):454–461
13. Seismosoft (2022) SeismoStruct 2022—a computer program for static and dynamic nonlinear analysis of framed structures. Available from https://seismosoft.com/
14. Shahnewaz M, Alam MS (2015) Seismic performance of reinforced concrete wall with superelastic shape memory alloy rebar. In: Structures congress 2015, pp 2230–2240
15. Tolou Kian MJ, Cruz-Noguez C (2018) Reinforced concrete shear walls detailed with innovative materials: seismic performance. J Compos Constr 22(6):04018052
16. Tran TA, Wallace JW (2012) Experimental study of nonlinear flexural and shear deformations of reinforced concrete structural walls. In: Proceedings of the 15th world conference on earthquake engineering, Lisbon, Portugal
17. Youssef MA, Alam MS, Nehdi M (2008) Experimental investigation on the seismic behavior of beam-column joints reinforced with superelastic shape memory alloys. J Earthq Eng 12:1205–1222